Send Orders for Reprints to reprints@benthamscience.ae

Open Chemistry Journal, 2016, *3*, 25-34 25

BENTHAM OPEN

CrossMark

Open Chemistry Journal

Content list available at: www.benthamopen.com/CHEM/

DOI: 10.2174/1874842201603010025

Design and Synthesis of a Multi Cu(II)-porphyrin Array

Virginia Gómez-Vidales[a], Andres Borja-Miranda[a], Sandra Cortez-Maya[a], Oscar Amelines-Sarria[b], Margarita Rivera[b] and Marcos Martínez-García[a,*]

[a]*Instituto de Química, Universidad Nacional Autónoma de México, Ciudad Universitaria, Mexico city, Mexico*
[b]*Instituto de Física, Universidad Nacional Autónoma de México, Ciudad Universitaria, Mexico city, Mexico*

Received: October 1, 2015 Revised: January 27, 2016 Accepted: January 30, 2016

Abstract: A new class of porphyrin array was synthesized. The Cu(II) porphyrin-PAMAM-Cu(II) porphyrin was obtained in good yields. The EPR studies showed that all porphyrins obtained have signals of a copper complex with planar geometry, and no variation in the tetrahedral distortion of the porphyrin ring was observed. The UV-vis and emission studies showed that the intensity of the signal increased due to the presence of 5 porphyrin moieties in the structure. In order to further characterize this molecule, thin films were prepared by using the thermal evaporation method. The morphology of the film showed a homogeneous structure while conductivity measurements exhibit a good conductive response.

Keywords: Conductivity, EPR, multi-porphyrin array, porphyrin.

1. INTRODUCTION

The design and synthesis of arrays of oligomeric porphyrins or metalloporphyrins having well-defined shapes and dimensions is currently a topic of great interest to improve the photophysical properties, absorption cross-section and directed energy-transfer reactions [1 - 3]. Metalloporphyrin or freeporphyrin arrays with different structures such as dendrimers of arylethynyl chromophores [4], self-assembling porphyrinic pigments [5 - 11] or metal coordination complexes [12, 13] containing five, nine or more porphyrins [14 - 22], have been used as an energy funnel, molecular photonic wires [13] or optoelectronic gates [23]. Recent development in synthesis strategies allows designing a variety of materials, mainly due to the possibility of changing the structure, porphyrin properties, number of porphyrins, interconnections and energy transfer. This diversity is of great importance in the obtainment of light-harvesting devices.

Here, we report a new method to obtain a flexible star PAMAM porphyrin pentamer in order to generate receptors able of binding, recognizing and transferring energy.

2. RESULTS AND DISCUSSION

The porphyrin core **1** and **4** were obtained from *para*-hydroxybenzaldehyde, benzaldehyde and pyrrole by the conventional method [24, 25]. The tetrahydroxyporphyrin was used as free based material. Metallation was performed by adding a suspension of copper (II) acetate in methanol to a solution of the free base porphyrin. The tetraester **2** was obtained from methyl bromoacetate with the phenol of the porphyrin **1** in acetone and K_2CO_3 as catalyst. Finally the amide **3** was prepared with ethylenediamine (Scheme **1**).

The porphyrin **4** was prepared according to reported methodology [25] and the copper (II) porphyrin 5 was obtained using $Cu(OAc)_2$, and this was modified with methyl bromoacetate in acetone and K_2CO_3 as catalyst, obtaining the monoester porphyrin **6** (Scheme **2**).

* Address correspondence to this author at the Instituto de Química, Universidad Nacional Autónoma de México, Ciudad Universitaria, Circuito Exterior, Coyoacán, C.P. 04510, México city, México; E-mail: margar@unam.mx

The ^{1}H-NMR spectrum of compound **6** exhibits: one singlet at δ_H 3.74 due the protons of O-CH_3 groups, at δ_H 4.22 due to the CH_2-O, two signals at δ_H 7.27, and δ_H 7.73 due to the AB system at the *para* substituted benzene group, and the signals at δ_H 7.31, 8.21 and 8.83 due to the aromatic and pyrrole protons.

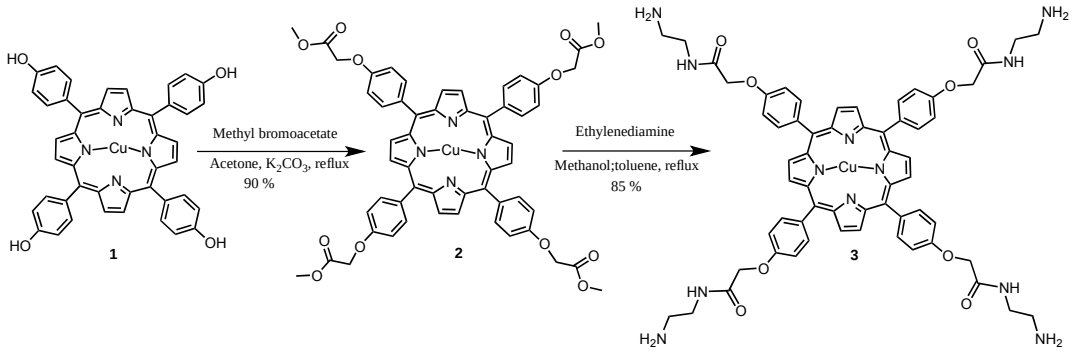

Scheme (1). Synthesis of the porphyrin-PAMAM dendrimer.

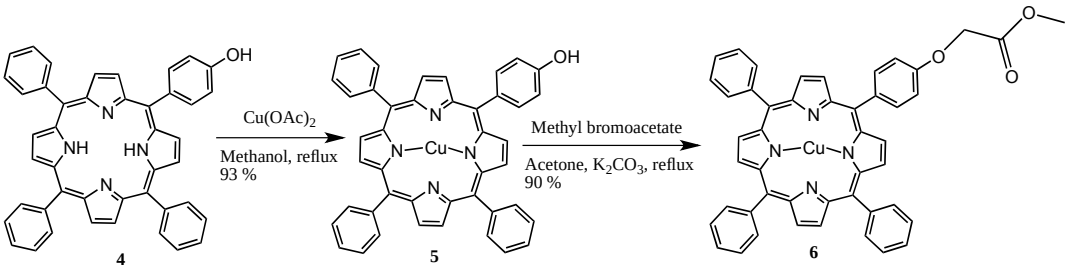

Scheme (2). Synthesis of the mono ester porphyrin.

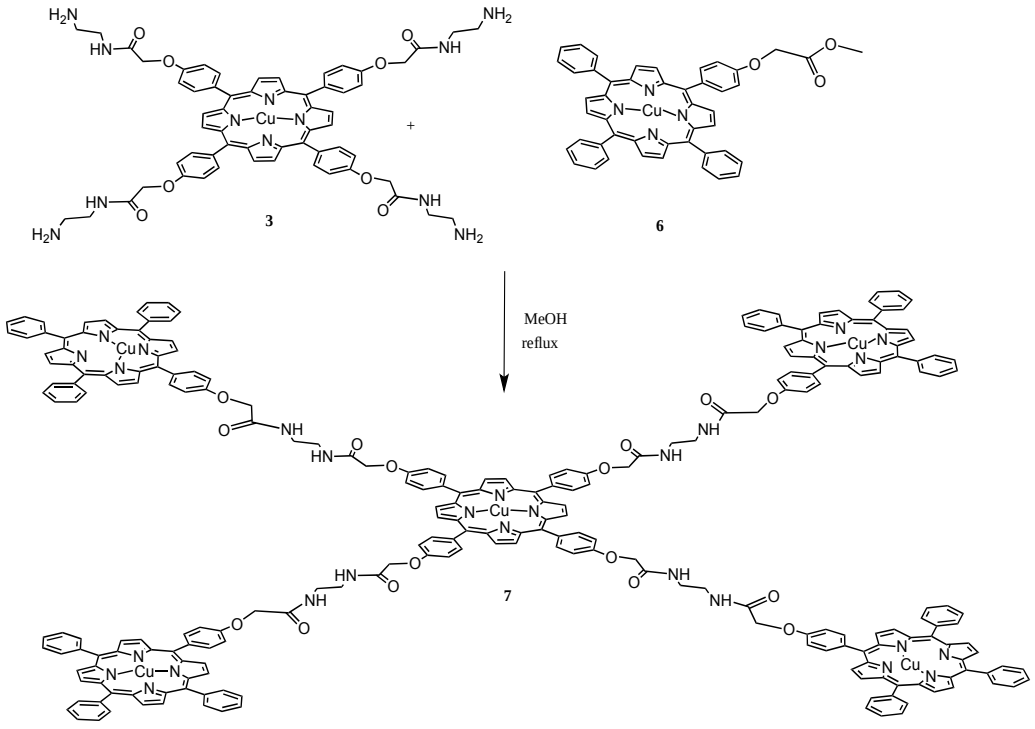

Scheme (3). Synthesis of the penta porphyrin array.

The pentamer was obtained in one step by an amidation reaction between the compounds **3** and **6** (Scheme **3**) in methanol at reflux for **4** hours giving compound **7** with a 35 % yield.

The ^{1}H-NMR spectra of compound **7** exhibits: two signals at δ_H 1.60 and at δ_H 2.95 for the N-H and ethyl protons, signals at δ_H 4,80 and 4.94 for the Ar-CH_2-O, and for the protons of the aromatic substituents seven signals at δ_H 7.08, 7.50, 7.66, 7.78, 7.98, 8.23, and at 8.59. And the beta pyrrolic protons at δ_H 8.83 were observed. The full functionalization of the porphyrin was corroborated by MALDI-TOF and is observed at 4064 *m/z* the mass of compound **7** (Fig. **1**).

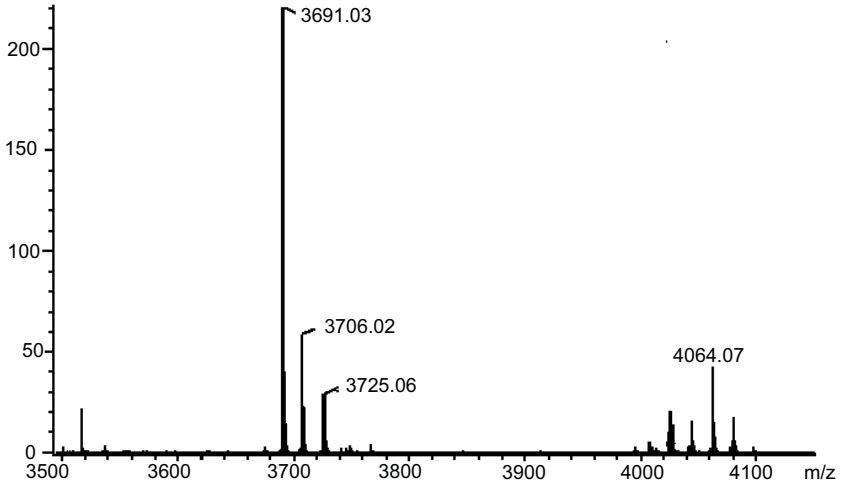

Fig. (1). MALDI-TOF mass spectra of the compound **7.**

2.1. Electron Paramagnetic Resonance (EPR) Studies

Porphyrins have delocalized π electrons. The EPR signals of these delocalized π electron systems are generated by the interaction of the porphyrin, or in the case of metal-porphyrins, by the unpaired electrons of a metal ion with the magnetic field (Fig. **2**).

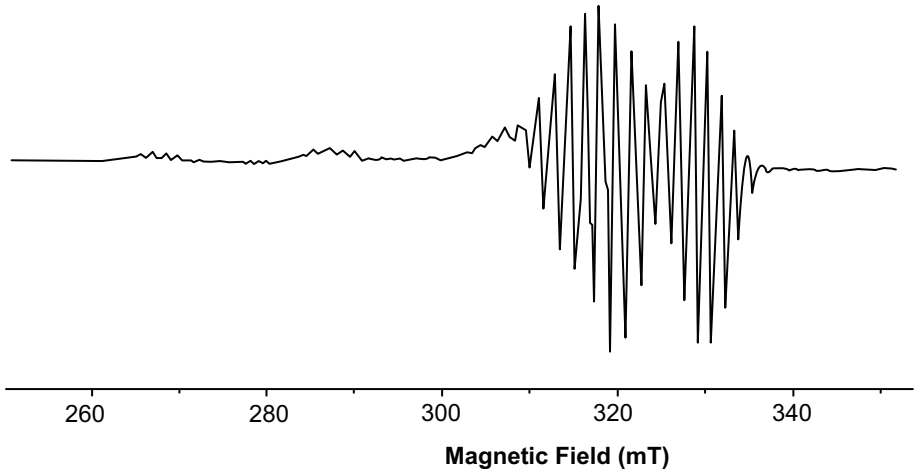

Fig. (2). Spectral behavior of the porphyrin **1**.

The copper porphyrin complex exhibits an anisotropic EPR spectra typical of copper (II) centers with well determined hyperfine lines in the $g_{I.}$ All signals show the dependence $g_{II} > g_{\perp} > ge$ which is diagnostic of a d_x^2-$_y^2$ ground state for copper (II), the hyperfine structure is obtained from the contact between delocalized π electrons and the nuclear spin I_{Cu}=3/2. The values obtained by simulated spectra are shown in Table **1**. Additionally, in the spectra, a super hyperfine structure can be observed due to the coupling of with the nuclei of pyrrole nitrogens of Cu-porphyrin I_N =1 (shfcc). The simulated spectra show the values in Table **1**.

The tetrahedral distortion that frequently occurs for square planar copper complexes is observed by the ratio $f = g_{\|}/A_{\|}$ and it is considered for the determination of the distortion and the deviation from perfect geometry depending on the coordinated ligands [26, 27]. The *f* value in the range 110-120 is typical for signals of the copper complex with planar geometry, however, its increase to 150 indicates a small or modest distortion of the planar symmetry, and the higher values, 180- 250, suggest a strong deviation from square planar geometry. In general, as a complex becomes more tetrahedral, the $g_{\|}$ value and the g_{iso} value increase and the A_{iso} and $A_{\|}$ values decrease [28]. Additionally, the EPR spectra can help with an estimation of the geometry that the compounds have adopted, by using the isotropic parameters $A_{iso} = (A_{\|} + 2A_{\perp})/3$ and $g_{iso} = (g_{\|} + 2g_{\perp})/3$. The values for planar symmetry are between A_{iso}= 75 -90 cm^{-1} and g_{iso}= 2.06 - 2.11 [29, 30].

Table 1. EPR data of porphyrins 1, 2, 3, 6 and 7 in methanol at 295 K and at 77 K.

Compound	g‖	$g^{\perp}$	A‖[a]	$A^{\perp}$ [a]	g_{iso}	A_{iso} [a]	α^2	shfcc	*f* [b]
1	2.1858	2.0598	206.13	17.3	2.1018	80.25	0.8207	16.5	106.03
2	2.1860	2.0610	206.15	17.3	2.1026	79.55	0.8215	16.5	106.03
3	2.1858	2.0520	205.11	17.3	2.0966	78.59	0.8145	16.5	106.56
6	2.1900	2.0612	206.53	9.6	2.1041	75.25	0.8284	16.5	106.03
7	2.1868	2.0640	206.22	17.4	2.1049	78.37	0.8238	16.5	106.03

[a] Coupling constants are in cm^{-1} and multiplied by 10^4; [b] The parameter *f* is given by $g_{\|}/ A_{\|}$; [c] The units are given in cm^{-1}, g+-0.002 y A+- 0.001.

The results show no variation in the tetrahedral distortion (Table **1**) among all compounds, since all the values are close to f = 106 cm^{-1} indicating a planar geometry. No increase in the tetrahedral distortion of the porphyrin ring was observed because of ring stiffness. The values found for g_{iso} (2.09 to 2.10) and A_{iso} 75 to 85 cm^{-1} are consistent with a square planar geometry.

2.2. Photophysical Studies in Solution

The absorption spectra of the metalloporphyrins **1**, **2**, **3**, **5**, **6** and **7** showed similar Soret or B and Q bands (Fig. **3**). A small ipsochromic change of the B band by a some nm can be perceived in the pentamer porphyrin array when compared to the monomeric porphyrin Cu(II), which signifies a faint excitonic coupling amid the subunits in the porphyrin, independent of the concentration (1 x 10^{-6} M^{-1} and 3 x 10^{-8} M^{-1}). The porphyrins are quite undisturbed and the porphyrins are alone mild electronically coupled [31].

The difference in the absorption intensity of the porphyrin-core derivatives **1-6** in comparison with the pentaporphyrin array is caused by the porphyrin substituents on the porphyrin-connected phenyl rings. As the porphyrin derivative size intensities, no shifts in the fluorescence and absorption bands were observed, indicating that the substituents, which are targeted outward from the porphyrin center, do not engage with the dyes [32]. Therefore, the substituents are not assumed to change either the character of the photoexcitation or the consequent photophysical processes of the porphyrin moiety.

When excited at 425 nm, all Cu-porphyrins emit at 605 nm and at 659 nm (Fig. **4**).

Table **2** shows the absorption spectral data of compounds **1-7** in CH_2Cl_2 at 24 °C, where the molar extinction coefficient (ε) of the absorbance of the compounds **1-7** showed an increase for the compounds **2-4**, and decrease for the compounds **5-7**, while the quantum yield showed slightly changes.

Table 2. Absorption, fluorescence profiles of porphyrins (1-7).

Compound	λ^{max} (nm)	ε x10^{-5} $M^{-1}.cm^{-1}$	Fluorescence λ max (nm)	Fluorescence quantum yield ϕ^F
1	409	1.15	652	0.6095
2	407	3.07	653	0.6095
3	415	2.00	652	0.5908
4	413	2.73	653	0.4695
5	415	1.57	655	0.5950
6	417	1.15	651	0.5998
7	415	1.14	651	0.5997

2.3. Morphological Film Properties

In Fig. (**5**), the surface morphology of the film from compound **7** is shown. From this image, a very regular distribution is observed. In addition, the surface coverage is complete which suggests a homogenous deposit on the ITO substrate.

The surface morphology was further analyzed using atomic force microscopy. In Fig. (**6**), an AFM image of compound **7**, is observed, which shows a granular aspect. From this image, it is clear that the surface coverage is not homogeneous, since small defects or holes can be seen irregularly distributed on the film surface. The thickness of the film was 30nm and the mean roughness value was 1.33 nm, which nevertheless, suggests the presence of a very flat film.

2.4. Conductivity Studies

In addition to the morphological characterization, the surface conductivity of the film of **7** was measured. In Fig. (**7**), a conductivity (V *vs.* I) plot of the bare ITO substrate and film in the presence and absence of light is shown. From these curves, the linear resistance of the bare ITO was calculated as 82.17 ohms, while the film shows a linear resistance of 43.05 ohms. This change suggests that the film exhibits a larger conductivity in comparison to the ITO substrate. In the presence of light, there is a slight decrease in linear resistance (42.02 ohms), which suggests a very small photoconductive response.

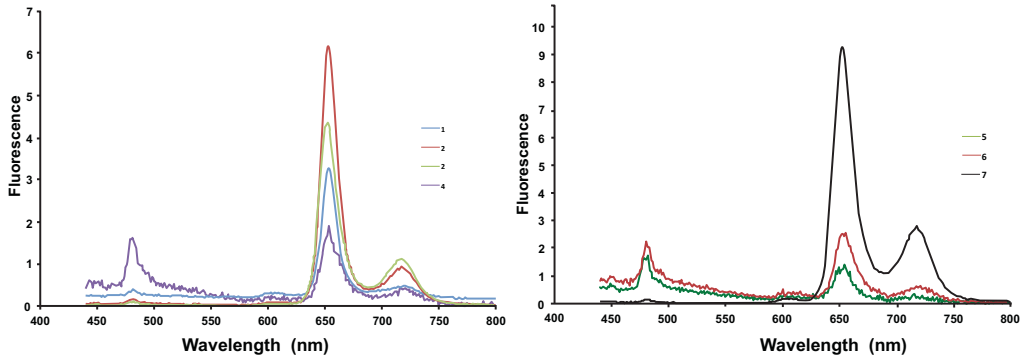

Fig. (3). Absorption spectra of the compounds **1**-**7** in CH_2Cl_2 at room temperature.

3. CONCLUSION

A new class of porphyrin array has been synthesized. The Cu(II) porphyrin-PAMAM-Cu(II) porphyrin was obtained in good yields. The EPR studies showed that all porphyrins obtained have signals of a copper complex with planar geometry, and no variation in the tetrahedral distortion of the porphyrin ring was observed. The UV-vis and emission studies showed that the intensity of the signal was increased due to the presence of five porphyrins in the structure. On the other hand, the Cu(II) porphyrin-PAMAM-Cu(II) porphyrin produced regular films when deposited onto ITO surfaces. The morphology showed a granular aspect with few scattered defects or vacancies. The photoconductive response of the film was not very large, possibly due to the irregularities on the film surface, which might affect the conduction paths or inefficient molecular packing due to the molecular geometry. Nevertheless, the conductivity of the film is larger than the one measured for the bare ITO surface, which suggests the presence of a conductive organic film.

4. EXPERIMENTAL SECTION

4.1. Materials and Equipment

Solvents and reagents were purchased as reagent grade. ^{1}H and ^{13}C NMR spectra were recorded on a Varian Unity-300 MHz in $CDCl_3$. The UV-Vis absorption and emission spectra were performed using a Shimadzu 2401 PC spectrophotometer and Perkin-Elmer LS-50 spectrofluorimeter. Quantum yields (ΦF) were determined using a quinine solution in CH_2Cl_2 as fluorescence standard (ΦF (std) = 0.546). All compounds were dissolved in dichloromethane (n = 1.445) and the fluorescence standard (n_{std}= 1.465). The EPR measurements were made in a Jeol JES-TE300 spectrometer. The g- factor values were calculated according to Weil [33]. The films for the photoelectric measurements were prepared on glass plates covered with a semitransparent layer of indium tin oxide (ITO) with a

sheet resistance of 10 ohms/sq. The substrates were cleaned and nitrogen was dried before each evaporation. The Cu(II) porphyrin-PAMAM-Cu(II) porphyrin compound was deposited by using a NORM vacuum thermal evaporator VCM 600 working at a 10^{-6} mbar pressure. The morphological properties of the film were evaluated with a JEOL FE7800F scanning electron microscope (SEM) working at 1kV in the gentle beam mode, in order to minimize the destruction and charging of the films. In addition, atomic force microscopy (AFM) images were obtained with a JEOL JSPM4210 instrument in the tapping mode to determine the morphology, thickness and roughness of the films.

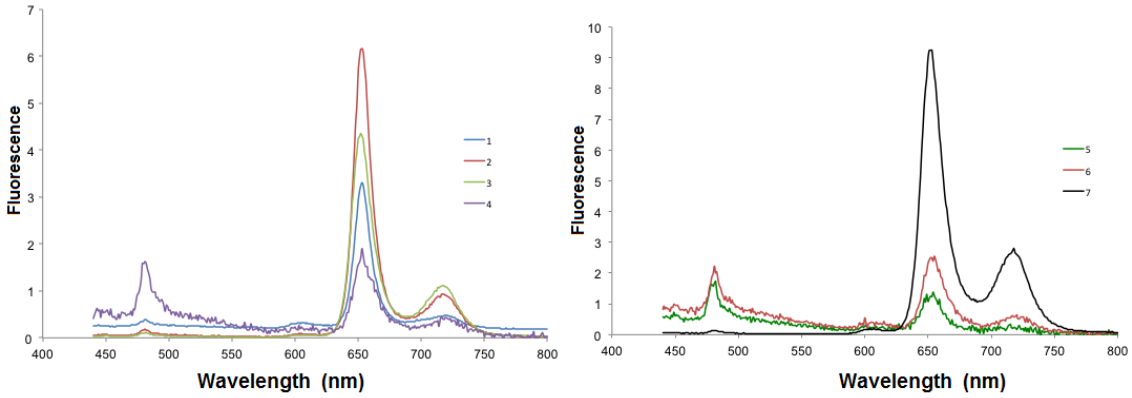

Fig. (4). Emission spectra of the compounds **1-7** in CH_2Cl_2 at room temperature.

The photoconductive response of the film was evaluated with a Keithley 2400 digital SourceMeter instrument and an Oriel LCS-100 solar simulator lamp with an AM1.5G filter.

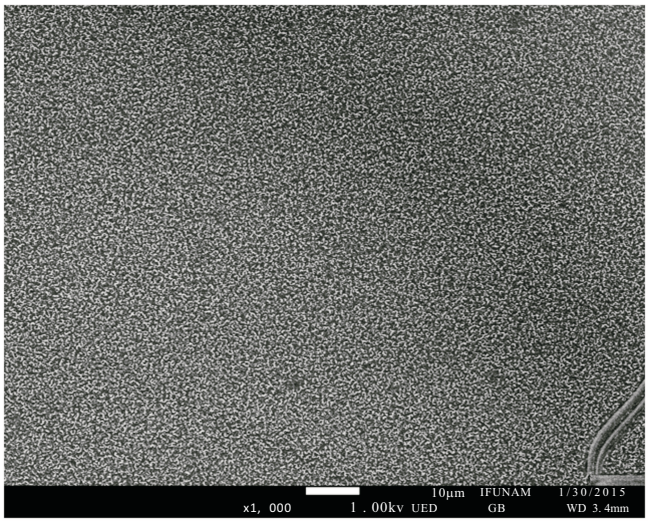

Fig. (5). SEM image of the metalloporphyrin film. Image magnification is 1,000X.

4.2. Synthesis

Copper porphyrin 1

5,10,15,20-tetrakis(4-hydroxyphenyl)-21H,23H-porphine 200 mg (0.294 mmol) and $Cu(OAc)_2$ 58 mg (0.294 mmol) were dissolved in methanol (20 mL), and refluxed for 4 h, then distilled water (60 mL) was added, and the methanol was evaporated under vacuum. The solution was cooled, and the purple crystalline product was obtained (0.28 mmol), FTIR (pellet, KBr, cm^{-1}): 3245, 1606, 1502, 1431, 1342, 1209, 1168, 999, 794, 719, 532. UV-vis (CH_2Cl_2): λ_{max} 417, 540 nm. ^1H NMR (300 MHz, in $CDCl_3$) δ_H: 6.62 (t, 4 H, Ar-H), 7.01 (d, 8 H, Ar-H), 8.86 (s, 8 H, Ar-H), 9.60 (s, 8 H, Ar-OH). ^{13}C NMR (75 MHz, in $CDCl_3$) δ_C: 101.72 (Ar-H). 114.16 (Ar), 120.23 (Ar), 131.33 (Ar), 156.21 (Ar-OH), 144.46 (Ar-porph), 148.93 (Ar), MS (FAB^+) *m/z*: 739 (M^+). Anal. Calcd for $C_{44}H_{28}CuN_4O_4$. C 71.39 %, H 3.81 %, Cu 8.58 %, N 7.57 %, O 8.65 %. Found: C, 71.40, H, 3.83, N, 7.57 %.

Compound 2

Methyl bromoacetate 22.8 mg (1.60 mmol) and potassium carbonate (3.20 mmol) in dry acetone (50 mL) were refluxed for 20 min. The PcCu(II) **1**, 122 mg (1.60 mmol) in dry acetone (40 mL) was added drop wise and stirred for 6 hours. The mixture was filtered. The filtrate was evaporated to dryness under pressure. The residue dissolved in diethyl ether and washed with a solution of 5% Na_2CO_3 in H_2O (3 times). The organic layer was evaporated to give the ester **2** (0.27 mmol) as a purple solid in 90 % yield. m.p: > 300 °C. FTIR (pellet, KBr, cm^{-1}): 2954, 2920, 1750, 1602, 1503, 1430, 1298, 1207, 1173, 1140, 1076, 963, 806, 708, 604, 593. UV-vis (CH_2Cl_2): λ_{max} 417, 540. ^{1}H NMR (300 MHz, $CDCl_3$) δ_H: 3.89 (br, 12H, O-CH_3), 4.82 (br, 8H, CH_2-O), 7.06 (br, 24H, Ar, pyrrol). ^{13}C NMR (75 MHz, $CDCl_3$) δ_C: 52.4 (CH_3-O), 65.4 (CH_2-O), 112.5 (Ar), 119.4 (Ar_{ipso}), 137.2 (pyrrol), 141.0 (Ar), 145.7 ($pyrrol_{ipso}$), 157.1 (Ar_{ipso}-O), 169.4 (C=O). MS (FAB$^+$) m/z: 1027 (M^+). Anal. Calcd for $C_{56}H_{44}CuN_4O_{12}$. C 65.40 %, H 4.31 %, Cu 6.18 %, N 5.45 %, O 19.85 %. Found: C, 65.43, H, 4.3, N, 5.42 %.

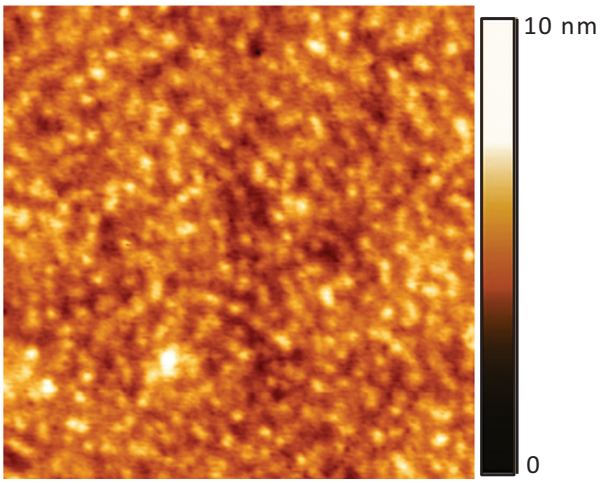

Fig. (6). AFM image of the metalloporphyrin film. Image size is 2 x 2 μm.

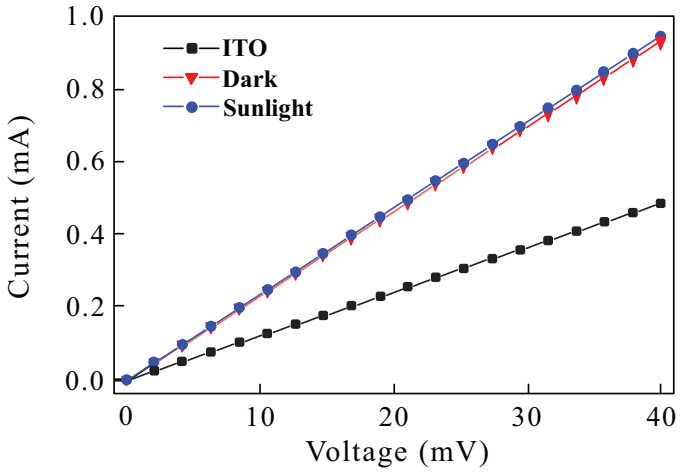

Fig. (7). V *vs.* I plots for the bare ITO surface and the porphyrin thin film in the presence and absence of light.

Compound 3

A mixture of ester-containing derivative **2** 190 mg (0.197 mmol) and ethylenediamine 81 mg (0.788 mmol) in methanol: toluene 1:1 was stirred and refluxed for 24 h. The solvents were removed in vacuo. The residue was washed several times with alcohol to obtain the amide compound **3** (0.16 mmol) as a purple solid in 85 % yield. m.p: > 300 °C. FTIR (pellet, KBr, cm^{-1}): 3302, 3032, 2917, 1655, 1602, 1533, 1498, 1343, 1284, 1225, 1174, 996, 799, 536. UV-vis (CH_2Cl_2): λ_{max} 417, 541, 682. ^{1}H NMR (300 MHz, $CDCl_3$) δ_H: 1.60 (br, 8H, NH_2), 3.90 (m, 16H, CH_2-NH_2), 4.83 (s, 8H,

CH_2-O), 7.06 (br, 24H, Ar, pyrrol). ^{13}C NMR (75 MHz, $CDCl_3$) δ_C: 52.4 (CH_2-NH_2), 65.5 (CH_2-O) 112.5 (Ar), 115.0 (Ar_{ipso}), 137.0 (pyrrol), 157.1 (Ar-O), 169.4 (C=O). MS (FAB^+) m/z: 1140 (M^+). Anal. Calcd for $C_{60}H_{60}CuN_{12}O_8$. C 63.17 %, H 5.30 %, Cu 5.57 %, N 14.73 %. Found: C, 63.19; H, 5.29, N 14.72 %.

5-(4-Hydroxyphenyl)-5,10,15-triphenyl-porphyrin 4

Benzaldehyde 2.08 g (0.02 mmol),) *para*-hydroxybenzaldehyde 2.45 g (0.02 mmol), and pyrrole 2.72 g (0.04 mmol) were added in propionic acid (15 mL) for 3 h. After the workup the reaction mixture was washed with water and chromatographed on a silica gel column using a mixture of hexane-ethyl acetate. Obtaining 4 0.23 g as a purple solid in 37 % yield. m.p: > 300 °C. FTIR (pellet, KBr, cm^{-1}): 3503, 3331, 2919, 1606, 1559, 1469, 1167, 793. UV-vis (CH_2Cl_2): λ_{max} 408, 515, 550, 590, 646. ^{1}H NMR (300 MHz, $CDCl_3$) δ_H: -2.79 (br, 2H, NH), 7.24 (d, 2H, Ar, J = 9.0 Hz), 8.16 (m, 6H, Ar), 8.09 (d, 2H, Ar, J= 9.0 Hz), 8.21-8.24 (m, 3H, Ar), 8.85 (m, 6H, Ar), 8.88 (br, 8H, pyrrol). ^{13}C NMR (75 MHz, $CDCl_3$) δ_C: 113.7 (Ar), 120.0 (Ar-porph), 126.0 (Ar), 127.7 (Ar), 131.0 (pyrrol), 134.5 (Ar), 140.3 (Ar), 142.2 ($pyrrol_{ipso}$), 143.2 (Ar-O). MS (FAB^+) m/z: 630 (M^+). Anal. Calcd for $C_{44}H_{30}N_4O$. C 83.79 %, H 4.79 %, N 8.88 %. Found: C, 83.77; H, 4.79, N 8.86 %.

Compound 5

A mixture of **4** 0. 1 g (0.158 mmol) and Cu(OAc)$_2$ 0.1 g (0.23 mmol) in methanol (20 mL), was heated to reflux for 4 h. Following the same methodology reported above, giving 5 0.150 g (0.21 mmol, yield 93 %). m.p: > 300 °C. FTIR (pellet, KBr, cm^{-1}): 3317, 2919, 1759, 1739, 1597, 1437, 1218, 1177, 795, 700. UV-vis (CH_2Cl_2): λ_{max} 408, 515, 550, 590, 646. ^{1}H NMR (300 MHz, $CDCl_3$) δ_H: 7.52 (br, 2H, Ar), 7.75 (br, 6H, Ar), 8.08 (br 2H, Ar), 8.21 (br, 3H, Ar), 8.87 (br, 6H, Ar), 8.88 (br, 8H, pyrrol). ^{13}C NMR (75 MHz, $CDCl_3$) δ_C: 113.7 (Ar), 120.0 (Ar-porph), 126.0 (Ar), 127.7 (Ar), 130.8 (pyrrol), 134.5 (Ar), 135.7 (Ar), 142.2 (Ar-O). MS (FAB^+) m/z: 692 (M^+). Anal. Calcd for $C_{44}H_{28}CuN_4O$. C 76.34 %, H 4.08 %, N 8.09 %. Found: C, 76.32; H, 4.09, N 8.06 %.

Compound 6

Methyl bromoacetate 0.241 g (1.60 mmol), potassium carbonate (3.20 mmol) dissolved in dry acetone (50 mL) and heated to reflux and stirred vigorously in a nitrogen atmosphere for 20 min**.** The compound **5** 0.110 g (1.60 mmol) dissolved in dry acetone (40 mL) was added drop wise and the reaction was continued for 6 hours. The mixture was filtered. The filtrate was dried under pressure. The monoester **6** was obtained following the same methodology used for the compound **3.** Obtaining 0.206 g (0.27 mmol) as a purple solid in 90 % yield. m.p: > 300 °C. FTIR (pellet, KBr, cm^{-1}): 3034, 2924, 1760, 1501, 1270, 1175, 1070, 996, 805, 702. UV-vis (CH_2Cl_2): λ_{max} 418, 540. ^{1}H NMR (300 MHz, $CDCl_3$) δ_H: 3.74 (s, 3H, O-CH_3), 4.22 (s, 2H, CH_2-O), 7.27 (br, 2H, Ar), 7.73 (br, 6H, Ar), 8.13 (br, 2H, Ar), 8.21 (br, 3H, Ar), 8.83 (br, 14H, Ar, pyrrol).^{13}C NMR (75 MHz, $CDCl_3$) δ_C: 52.3 (O-CH_3), 68.10 (CH_2-O), 112.9 (Ar), 120.1 (Ar-porph), 126.6 (Ar), 127.1 (Ar_{ipso}) 127.7 (Ar), 130.8 (pyrrol), 134.5 (Ar), 135.6 (Ar), 142.2 (Ar-O), 170.0 (C=O). MS (FAB^+) m/z: 763 (M^+). Anal. Calcd for $C_{47}H_{32}CuN_4O_3$. C 73.86 %, H 4.22 %, N 7.33 %. Found: C, 73.84; H, 4.23, N 7.31 %.

Compound 7

The compound **6** 100 mg (0.144 mmol) and the amide compound **3** 114 mg (0.144 mmol) were dissolved in methanol (20 mL). The mixture was heated to reflux for 4 h, and then the methanol was evaporated under vacuum. The purple crystalline product was dried *in vacuo* at 40 °C (yield 35 %). m.p: > 300 °C. FTIR (pellet, KBr, cm^{-1}): 3033, 2920, 2850, 1727, 1600, 1499, 1213, 1174, 1071, 798, 703. UV-vis (CH_2Cl_2): λ_{max} 413, 449, 540, 622, 776. ^{1}H NMR (300 MHz, $CDCl_3$) δ_H: 1.60 (br, 8H, NH), 2.95 (m, 16H, CH_2-NH), 4.80 (s, 8H, CH_2-O), 4.94 (s, 8H, CH_2-O), 7.08 (br, 8H, Ar), 7.50 (br, 8H, Ar), 7.66 (br, 24H, Ar), 7.78 (br, 8H, Ar), 7.98 (br, 8H, Ar), 8.23 (br, 12H, Ar), 8.59 (br, 24H, Ar), 8.83 (br, 40H, pyrrol). ^{13}C NMR (75 MHz, $CDCl_3$) δ_C: 49.1 (CH_2-NH_2), 65.2 (CH_2-O) 112.5 (Ar), 115.0 (Ar_{ipso}), 126.3 (Ar), 126.7 (Ar), 127.0 (Ar), 128.2 (Ar), 137.0 (pyrrol), 157.1 (Ar-O), 171.0 (C=O). MALDI-TOF m/z: 4064 (M^+). Anal. Calcd for $C_{244}H_{172}Cu_5N_{28}O_{16}$. C 72.01 %, H 4.26 %, N 9.64 %. Found: C, 72.00; H, 4.28, N 9.63 %.

CONFLICT OF INTEREST

The authors confirm that this article content has no conflict of interest.

ACKNOWLEDGEMENTS

This work was supported by the DGAPA-UNAM (IN-107814) grant. MR acknowledges DGAPA-UNAM IN-106513 grant. O. Amelines-Sarria acknowledges financial support from DGAPA CJIC/CTIC/1334/2013. We would also like to thank Rios O. H., Velasco L., Huerta S. E., Patiño M. M. R., Peña Gonzalez M. A., Garcia Rios E. and Magaña Zavala C.R. for technical assistance.

REFERENCES

[1] Chen, C.T. *In Comprehensive Supramolecular Chemistry: Coordination Polymers*; Pergamon Press: New York, **1996**, vol. 5, no. 4, p. 91.

[2] Sanders, J.K. *The Porphyrin Handbook*; Kadish, K.M.; Smith, K.M.; Guilard, R., Eds.; Academic Press: New York, **2000**, vol. 3, p. 347.

[3] Ward, M.D. Photo-induced electron and energy transfer in non-covalently bonded supramolecular assemblies. *Chem. Soc. Rev.,* **1997**, *26*, 365-375.
[http://dx.doi.org/10.1039/cs9972600365]

[4] Xu, Z.; Moore, J.S. Design and synthesis of a convergent and directional molecular antenna. *Acta Polym.,* **1994**, *45*, 83-87.
[http://dx.doi.org/10.1002/actp.1994.010450204]

[5] Drain, C.M.; Lehn, J.M. Self-assembly of square multiporphyrin arrays by metal ion coordination. *J. Chem. Soc. Chem. Commun.,* **1994**, *24*, 2313-2315.
[http://dx.doi.org/10.1039/c39940002313]

[6] Chi, X.; Guerin, A.J.; Haycock, R.A.; Hunter, C.A.; Sarson, L.D. The thermodynamics of self-assembly. *J. Chem. Soc. Chem. Commun.,* **1995**, 2567-2569.
[http://dx.doi.org/10.1039/c39950002567]

[7] Miyaji, H.; Kobuke, Y.; Kondo, J. Molecular organization of mono(p-hydroquinonyl) porphyrin through coordinate bond. *Chem. Lett.,* **1996**, *6*, 497-498.
[http://dx.doi.org/10.1246/cl.1996.497]

[8] Tamiaki, H.; Amakawa, M.; Shimono, Y.; Tanikaga, R.; Holzwarth, A.R.; Schaffner, K. Synthetic zinc and magnesium chlorin aggregates as models for supramolecular antenna complexes in chlorosomes of green photosynthetic bacteria. *Photochem. Photobiol.,* **1996**, *63*, 92-99.
[http://dx.doi.org/10.1111/j.1751-1097.1996.tb02997.x]

[9] Alessio, E.; Macchi, M.; Heath, S.; Marzilli, L. G. A novel open-box shaped pentamer of vertically linked porphyrins that selectively recognizes S-bonded Me_2SO complexes. *Chem. Commun. (Camb.),* **1996**, 1411-1412.
[http://dx.doi.org/10.1039/cc9960001411]

[10] Kariya, N.; Imamura, T.; Sasaki, Y. Synthesis, characterization, and spectral properties of new perpendicularly linked osmium(II) porphyrin oligomers[1]. *Inorg. Chem.,* **1997**, *36*, 833-839.
[http://dx.doi.org/10.1021/ic960878k]

[11] Denti, G.; Serroni, S.; Campagna, S.; Juris, A.; Balzani, V. Small-upward approach to nanostructures-dendritic polynuclear metal-complexes for light-harvesting. *Mol. Cryst. Liq. Cryst. (Phila. Pa.),* **1993**, *234*, 79-88.
[http://dx.doi.org/10.1080/10587259308042900]

[12] Bothner-By, A.A.; Dadok, J.; Johnson, T.E.; Lindsey, J.S. Molecular dynamics of covalently-linked multi-porphyrin arrays. *J. Phys. Chem.,* **1996**, *100*, 17551-17557.
[http://dx.doi.org/10.1021/jp961408e]

[13] Wagner, R.W.; Lindsey, J.S. A molecular photonic wire. *J. Am. Chem. Soc.,* **1994**, *116*, 9759-9760.
[http://dx.doi.org/10.1021/ja00100a055]

[14] Anderson, S.; Anderson, H.L.; Bashall, A.; McPartlin, M.; Sanders, J.K. Assembly and crystal structure of a photoactive array of five porphyrins. *Angew. Chem. Int. Ed. Engl.,* **1995**, *34*, 1096-1099.
[http://dx.doi.org/10.1002/anie.199510961]

[15] Drain, C.M.; Russell, K.C.; Lehn, J.M. Self-assembly of a multi-porphyrin supramolecular macrocycle by hydrogen bond molecular recognition. *Chem. Soc. Chem. Commun. (Camb.),* **1996**, 337-338.
[http://dx.doi.org/10.1039/cc9960000337]

[16] Huck, W.T.; Rohrer, A.; Anilkumar, A.T.; Fokkens, R.H.; Nibbering, N.M.; van Veggel, F.C.; Reinhoudt, D.N. Non-covalent synthesis of multiporphyrin systems. *New J. Chem.,* **1998**, *22*, 165-168.
[http://dx.doi.org/10.1039/a708323h]

[17] Drain, C.M.; Nifiatis, F.; Vasenko, A.; Batteas, J.D. Porphyrin tessellation by design: metal-mediated self-assembly of large arrays and tapes. *Angew. Chem. Int. Ed.,* **1998**, *37*, 2344-2347.
[http://dx.doi.org/10.1002/(SICI)1521-3773(19980918)37:17<2344::AID-ANIE2344>3.0.CO;2-B]

[18] Kumar, R.K.; Goldberg, I. Supramolecular assembly of heterogeneous multiporphyrin arrays-structures of [{ZnII(tpp)}2(tpyp)] and the coordination polymer [{[MnIII(tpp)]2(tpyp)(ClO4)2}∞]. *Angew. Chem. Int. Ed.,* **1998**, *37*, 3027-3030.
[http://dx.doi.org/10.1002/(SICI)1521-3773(19981116)37:21<3027::AID-ANIE3027>3.0.CO;2-N]

[19] Taylor, P.N.; Anderson, H.L. Cooperative self-assembly of double-strand conjugated porphyrin ladders. *J. Am. Chem. Soc.,* **1999**, *121*, 11538-11548.
[http://dx.doi.org/10.1021/ja992821d]

[20] Solladié, N.; Gross, M.; Gisselbrecht, J.P.; Sooambar, C. Pentaporphyrin with flexible, chiral nucleosidic linkers: unexpected duality of the physico-chemical properties of its core. *Chem. Commun. (Camb.),* **2001**, *21*(21), 2206-2207.
[http://dx.doi.org/10.1039/b106337p] [PMID: 12240113]

[21] Flamigni, L.; Talarico, A.M.; Ventura, B.; Marconi, G.; Sooambar, C.; Solladié, N. Conformational effects on the photoinduced energy transfer in a star-shaped pentaporphyrin with nucleosidic linkers. *Eur. J. Inorg. Chem.,* **2004**, *12*, 2557-2569.
[http://dx.doi.org/10.1002/ejic.200300918]

[22] Solladié, N.; Sooambar, C.; Herschbach, H.; Strub, J.M.; Leize, E.; Van Dorsselaer, A.; Talarico, A.M.; Ventura, B.; Flamigni, L. A photoactive nona-porphyrin with nucleosidic linkers. *New J. Chem.,* **2005**, *29*, 1504-1507.
[http://dx.doi.org/10.1039/b509913g]

[23] Wagner, R.W.; Lindsey, J.S.; Seth, J.; Palaniappan, V.; Bocian, D.F. Molecular optoelectronic gates. *J. Am. Chem. Soc.,* **1996**, *118*, 3996-3997.
[http://dx.doi.org/10.1021/ja9602657]

[24] James, D.A.; Arnold, D.P.; Parsons, P.G. Potency and selective toxicity of tetra(hydroxyphenyl)- and tetrakis(dihydroxyphenyl)porphyrins in human melanoma cells, with and without exposure to red light. *Photochem. Photobiol.,* **1994**, *59*(4), 441-447.
[http://dx.doi.org/10.1111/j.1751-1097.1994.tb05062.x] [PMID: 8022886]

[25] Vaijanthimala, G.; Krishnan, V.; Mandal, S.K. Cyclic porphyrin dimers as hosts for coordinating ligands. *J. Chem. Sci.,* **2008**, *120*, 115-129.
[http://dx.doi.org/10.1007/s12039-008-0014-3]

[26] Labanova, M.; Bidzinska, E.; Para, A. EPR investigation of Cu(II)-complexes with nitrogen derivatives of dialdehyde starch. *Carbohydr. Polym.,* **2012**, *87*, 2605-2613.
[http://dx.doi.org/10.1016/j.carbpol.2011.11.034]

[27] Pogni, R.; Baratto, M.C.; Diaz, A.; Basosi, R.J. *Inorg. Biochemistry,* **2000**, *79*, 333-339.
[http://dx.doi.org/10.1016/S0162-0134(99)00166-X]

[28] Cline, S.J.; Wasson, J.R.; Hatfield, W.E.; Hodgson, D.J. Structure and spectroscopic properties of bis(N-cyclohexyl-3-methoxysalicylideneiminato)-copper(II). *J. Chem. Soc., Dalton Trans.,* **1978**, 1051-1057.
[http://dx.doi.org/10.1039/dt9780001051]

[29] Suresh, E.; Bhadbhade, M.M.; Srinivas, D. Molecular association, chelate conformation and reactivity correlations in substituted o-phenylenebis (salicylidenato) copper(II) complexes: UV-visible, EPR and X-ray structural investigations. *Polyhedron,* **1996**, *15*, 4133-4144.
[http://dx.doi.org/10.1016/0277-5387(96)00178-7]

[30] Joseph, M.; Kuriakose, M.; Kurup, M.R.; Suresh, E.; Kishore, A.; Bath, S.G. Structural, antimicrobial and spectral studies of copper(II) complexes of 2-benzoylpyridine N(4)-phenyl thiosemicarbazone. *Polyhedron,* **2006**, *25*, 61-70.
[http://dx.doi.org/10.1016/j.poly.2005.07.006]

[31] Holten, D.; Bocian, D.F.; Lindsey, J.S. Probing electronic communication in covalently linked multiporphyrin arrays. A guide to the rational design of molecular photonic devices. *Acc. Chem. Res.,* **2002**, *35*(1), 57-69.
[http://dx.doi.org/10.1021/ar970264z] [PMID: 11790089]

[32] Falk, J.E. *Porphyrins and Metalloporphyrins*; Elsevier: New York, **1964**, pp. 85-87.

[33] Weil, J.A.; Bolton, J.R. *Electron Paramagnetic Resonance*; Wiley Interscience: New York, **2007**.